LETTERS
PUBLISHED ONLINE: 20 APRIL 2015 | DOI: 10.1038/NCLIMATE2616
nature climate change

Physiological advantages of dwarfing in surviving extinctions in high-CO_2 oceans

Vittorio Garilli[1]*†, Riccardo Rodolfo-Metalpa[2,3]*†, Danilo Scuderi[4], Lorenzo Brusca[5], Daniela Parrinello[6], Samuel P. S. Rastrick[7], Andy Foggo[8], Richard J. Twitchett[9], Jason M. Hall-Spencer[8] and Marco Milazzo[10]

Excessive CO_2 in the present-day ocean–atmosphere system is causing ocean acidification, and is likely to cause a severe biodiversity decline in the future[1], mirroring effects in many past mass extinctions[2–4]. Fossil records demonstrate that organisms surviving such events were often smaller than those before[5,6], a phenomenon called the Lilliput effect[7]. Here, we show that two gastropod species adapted to acidified seawater at shallow-water CO_2 seeps were smaller than those found in normal pH conditions and had higher mass-specific energy consumption but significantly lower whole-animal metabolic energy demand. These physiological changes allowed the animals to maintain calcification and to partially repair shell dissolution. These observations of the long-term chronic effects of increased CO_2 levels forewarn of changes we can expect in marine ecosystems as CO_2 emissions continue to rise unchecked, and support the hypothesis that ocean acidification contributed to past extinction events. The ability to adapt through dwarfing can confer physiological advantages as the rate of CO_2 emissions continues to increase.

The present rate of ocean acidification is a global concern because many of the mass extinction events that affected evolution of life on Earth are associated with evidence for elevated CO_2 and global warming, triggered by large-scale continental volcanism[3]. These include the largest known extinction event, which occurred in the late Permian[2,8], where atmospheric CO_2 levels are estimated to have increased by a factor of four to six[9,10], and the Late Triassic event that saw a doubling in CO_2 levels[4] and was the most severe extinction to have affected extant groups such as scleractinian corals[11]. Evidence that ocean acidification due to volcanism played a significant role in past marine extinctions comes from analyses of physiological selectivity[12], and changes in shell mineralogy and lithology[13]. In the immediate aftermath of the mass extinction events, many of the survivors were smaller than before[5] (for example, brachiopods[14], gastropods[14], bivalves and shelled cephalopods[6]); a phenomenon termed the 'Lilliput effect'[7]. After the most severe Late Permian extinction, gastropod species remained relatively small for millions of years[15]. One hypothesis is that this dwarfing was an adaptation to ocean acidification to mitigate against the increased energetic cost of carbonate secretion[8]. Calcifiers use the ion transporter Ca^{2+} ATPase to build shells/skeletons which pumps protons out of the extracellular calcifying medium, increasing the internal pH and favouring calcification. This is an energetically expensive process[16], the cost of which increases for animals exposed to high p_{CO_2} conditions. For instance, scleractinian corals have an extra metabolic cost of about 10% per 0.1 unit decrease in seawater pH (ref. 17). It is possible that faced with an increase in calcification costs, some species may adapt by decreasing in size[18].

Areas with naturally high levels of CO_2 provide opportunities to study the adaptation of organisms exposed to chronic hypercapnia[19,20]. At such sites, increased CO_2 levels cause biodiversity loss on sufficiently large spatial and temporal scales to reveal ocean acidification effects at the ecosystem level[21,22]. Off Vulcano Island, Sicily[23], seep gas composition is 97–98% CO_2, which acidifies the surrounding waters down to pH_T 5.64 (where pH_T is the pH value based on the total hydrogen ion concentration scale) near the main seeps, rising to ambient levels of pH_T 8.2 over a distance of around 400 m (ref. 23). Traces of other hydrothermal gases (H_2, CH_4 and H_2S) are also present near the seeps but become undetectable around 5 m away[23]. Seawater temperature and oxygen levels reach ambient values a few tens of metres from the main seep area. At about 100 m from the main seeps the nassariid gastropods *Nassarius corniculus* and *Cyclope neritea* are abundant on coarse sand and gravel (Fig. 1). These species are widespread in coastal lagoons and salt marshes in the Mediterranean as well as at shallow-water hydrothermal seeps (for example, off Milos[24] and Pantelleria[25]). We know that populations of *C. neritea* and *N. corniculus* had developed at the CO_2 seeps because their shells had paucispiral protoconches indicating these snails lack a planktotrophic larval stage (see Supplementary Information for more details). Seawater off Vulcano has been acidified since the late Pleistocene epoch[23] and a dwarf population of *N. corniculus* has been present for at least 30 years[25], providing an opportunity to study chronic effects of ocean acidification on gastropods submitted to high CO_2 levels over multiple generations.

Here, we compared gastropods living in naturally acidified shallow-water conditions near CO_2 seeps off Vulcano with those

[1]APEMA—Paleosofia, Research & Educational Service, Via Alla Falconara 34, 90136 Palermo, Italy. [2]UMR ENTROPIE—Laboratoire d'Excellence CORAIL, Institut de Recherche pour le Développement, BP A5, 98848 Nouméa cedex, New Caledonia. [3]IAEA EL—International Atomic Energy Agency, Environmental Laboratories, 4 Quai Antoine 1er, 98000, Principality of Monaco. [4]BIOMLG—Department of Biological, Geological and Environmental Sciences, University of Catania, Via Mauro de Mauro 15b, Piano Tavola, 95032 Belpasso, Catania, Italy. [5]INGV—Istituto Nazionale di Geofisica e Vulcanologia, Sezione di Palermo, Via Ugo La Malfa, 153, 90146 Palermo, Italy. [6]STEBICEF—Dipartimento di Scienze e Tecnologie Biologiche Chimiche e Farmaceutiche, Università degli studi di Palermo, Via Archirafi 18, 90123 Palermo, Italy. [7]IMR—Institute of Marine Research, PO Box 1870 Nordnes, 5817 Bergen, Norway. [8]MBERC—Marine Biology and Ecology Research Centre, School of Marine Science and Engineering, Plymouth University, Drake Circus, Plymouth PL4 8AA, UK. [9]NHM—Natural History Museum, Cromwell Road, London SW7 5BD, UK. [10]DiSTeM—Department of Earth and Marine Sciences, University of Palermo, Via Archirafi 28, 90123 Palermo, Italy. †These authors contributed equally to this work.
*e-mail: vittoriogarilli@apema.eu; riccardo@rodolfo-metalpa.com

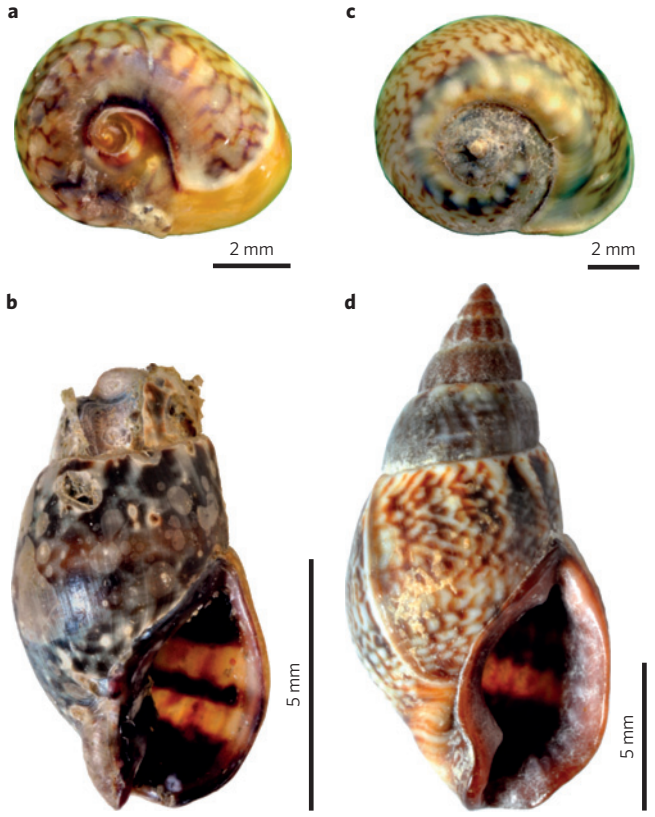

Figure 1 | Shells of the investigated species. a–d, Samples of *Cyclope neritea* (**a**,**c**) and *Nassarius corniculus* (**b**,**d**) living at CO_2 seeps (**a**,**b**) showing shell dissolution and apex truncation when compared to shells collected at reference site C1, ambient pH (**c**,**d**).

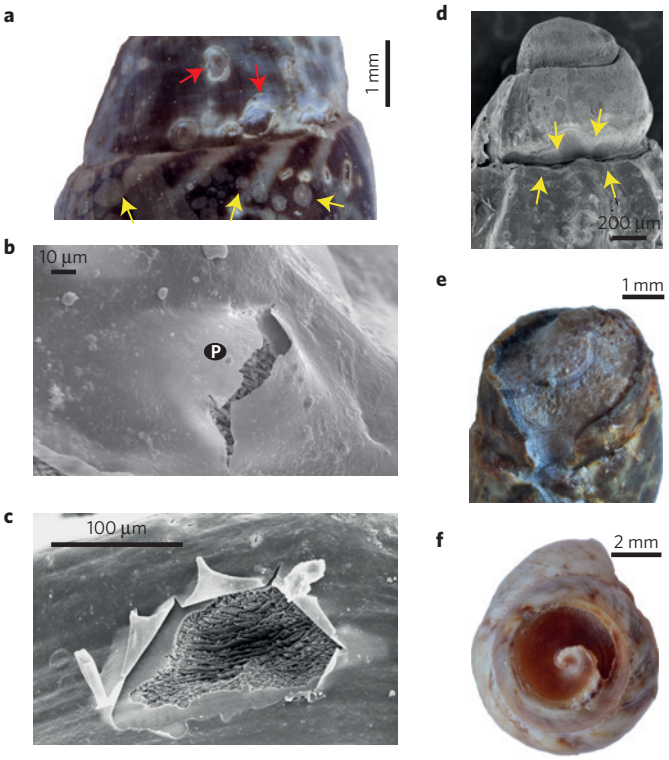

Figure 2 | Shell dissolution, apical truncation and repairing calcification process in *Nassarius corniculus* living at CO_2 seeps. a, Dissolution first affects shell periostracum (yellow arrows) and then mineralized shell layers (red arrows). **b**,**c**, Scanning electronic microscopy images showing shell periostracum (P) fractures (**b**), followed by shell dissolution (**c**). **d**, Juvenile specimen preserving the paucispiral protoconch, and showing dissolution of the sutural area (arrows) as a first step towards shell apical truncation. **e**, Adult specimen from CO_2 seeps showing a marked effect of dissolution. Although it lacks a shell apex, the animal was able to repair its shell, closing the internal cavity (see also Supplementary Figs 3 and 4). **f**, Shell cross-section of a sample from reference site C1 artificially broken to show the normal empty space between the outer part of the shell and the columella.

at sites with ambient seawater pH (Supplementary Fig. 1) to test for their ability to cope with acidification and, potentially, adapt. Shell morphology, dissolution and repair were examined using scanning electron microscopy. Animals collected in September and November 2011 were incubated in aquaria at CO_2 levels similar to those measured at reference and CO_2 seep sites (Supplementary Table 1) and their gross calcification rates[20] were measured using ^{45}Ca at both seawater pH levels. Rates of metabolic oxygen uptake of individuals from CO_2 seeps and a reference site were determined by stop-flow respirometry at pH_{NBS} 6.5 or pH_{NBS} 8.1, respectively, within 24 h of collection.

Gastropods were collected from the seep site at mean pH_T 7.41 ± 0.13 (corresponding to Ω_{ara} of 1.10 ± 0.28; Supplementary Table 1) where seawater pH varied during a 24-h cycle from about 6.6 to 7.7 pH_T units (Supplementary Fig. 2) and from three sites at pH_T 8.1. Considerably fewer specimens of both species were found at reference sites (on average 1 specimen m^{-2} versus 7 m^{-2}). Overall shell shapes were significantly different between sites (GLM $p < 0.001$, Supplementary Tables 2–13; PERMANOVA $p < 0.001$, Supplementary Tables 14–15) and individuals within species were significantly smaller at CO_2 seeps than at control sites, showing 1.26 and 1.37 mean (log) volume ratios between ambient and acidified conditions (see Table 1 for raw data; Tukey's LSD tests for Vulcano (acidified) versus ambient controls $p < 0.001$, Supplementary Tables 6 and 13). These shell volume shifts, which approximate to biomass shifts, provide a means of directly comparing experimental and fossil data[15]. In his global study of clade-level size change in gastropods Payne[15] recorded a shell volume shift of 1.45 mean (log) volume between the Late Permian and Early Triassic periods, which is of the same order as that recorded by our experimental data (Supplementary Fig. 3).

In *N. corniculus*, shell integrity was clearly affected by the corrosive seawater at CO_2 seeps; pockmarks were present on the teleoconch in almost all samples (Fig. 2a), corresponding to zones where the periostracum was affected by swelling and breaking (Fig. 2b). Deterioration of the periostracum is the first step before mineralized shell layers undergo dissolution (Fig. 2c), as previously shown in mussels at shallow[20] and deep CO_2 seeps[26]. For *C. neritea* the early shell whorls were also corroded at the CO_2 seeps, with loss of the protoconch and pitting on the first teleoconch whorl (Fig. 1a).

At reference sites, fully grown *N. corniculus* had 7–7.5 whorls, whereas all the *N. corniculus* collected at CO_2 seeps had only 1–2 whorls (Fig. 1b and Supplementary Fig. 4). Acidic environment gradually corroded gastropod shells, especially in the sutural area (Fig. 2d), suggesting that different truncations might affect a single individual during its life history. Although similar shell truncation is recorded in fossil gastropods from other seep environments[27], it is difficult to assess whether shell damage due to corrosive seawater was a common feature in gastropods surviving past extinctions[8], because shell dissolution may also occur post mortem, through fossilization processes as well as during collection and separation of the fossils from the rock.

Table 1 | Mean and standard deviation of shell morphometric parameters, shell volume and average size decrease of *Cyclope neritea* and *Nassarius corniculus* from CO_2 seeps and from reference sites C1–C3 (Stagnone di Marsala; Lampedusa Island; San Giovanni Li Cuti, respectively).

Data	Ht	Hlw	W	Ws	Ha	Olt	V	log V
Cyclope neritea								
CO_2 seep	3.47	3.23	6.97	-	4.28	0.71	44.6	1.64
(± s.d.)	(0.25)	(0.19)	(0.53)		(0.37)	(0.15)	(8.89)	
Reference C1	5.92	5.50	10.72	-	6.13	1.27	180.6	2.25
(± s.d.)	(0.41)	(0.36)	(0.91)		(0.50)	(0.21)	(41.3)	
Size decrease (%)								
CO_2 seep versus C1	41.4	41.3	35.0	-	30.0	43.3	75.3	26.9
Nassarius corniculus								
CO_2 seep	-	6.99	4.90	3.38	4.62	0.53	95.7	1.98
(± s.d.)		(0.24)	(0.26)	(0.17)	(0.33)	(0.06)	(12.1)	
Reference C1	-	10.35	7.87	5.60	7.67	0.95	377.5	2.57
(± s.d.)		(0.82)	(0.46)	(0.42)	(0.29)	(0.07)	(78.3)	
Reference C2	-	10.17	7.07	5.74	7.33	0.88	335.5	2.51
(± s.d.)		(0.98)	(0.72)	(0.60)	(0.60)	(0.16)	(86.9)	
Reference C3	-	9.51	6.89	7.17	7.17	1.03	286.5	2.45
(± s.d.)		(0.61)	(0.43)	(0.52)	(0.52)	(0.25)	(51.0)	
Size decrease (%)								
CO_2 seep versus C1		32.4	37.7	39.8	39.8	44.2	74.6	22.9
CO_2 seep versus C2		31.3	30.7	37.0	37.0	39.8	71.5	21.2
CO_2 seep versus C3		26.5	28.9	37.4	35.5	48.5	66.6	19.3

Shell morphometric parameters (given in mm) are: (Ht) total height; (Hlw) last whorl height; (W) last whorl width; (Ws) width at the suture between last and penultimate whorl; (Ha) aperture height; (Olt) outer lip thickness. For *N. corniculus*, Ht was not measured because all the Vulcano adult shells were to a lesser or greater extent truncated in their apical part. Volume (V) is in mm^3. The last whorl width (Ws) was measured only for *N. corniculus*, allowing calculation of volume by approximating shells as a truncated cone (see Supplementary Information for more details). For *C. neritea* $n = 25$ for both CO_2 seeps and reference site C1, whereas for *N. corniculus* $n = 40$ (seeps and reference site C1); $n = 20$ and 10 for reference sites C2 and C3 respectively.

In all of the *N. corniculus* specimens from CO_2 seeps the most severe surface injuries and the truncated apices were neatly plugged by a calcareous mass (Fig. 2e and Supplementary Fig. 5), presumably to protect the animal within and isolate the inner extrapallial fluid from the surrounding seawater. This repair calcification consisted of a thin layer (15–20 μm) of small prismatic elements (Supplementary Fig. 4) of similar size and orientation to those forming the outermost mineralized layer. Therefore, despite living in seawater undersaturated with carbonate, these molluscs were able to deposit new $CaCO_3$ to repair their shells.

In aquaria, the two species had positive gross calcification rates at both pH_T 8.1 and 7.2 (Fig. 3a), with higher rates in September than in November (GLM $p < 0.001$, Supplementary Table 16a), probably owing to seasonal differences in the environmental parameters between seasons, including seawater temperature. Gross calcification rates in *N. corniculus* collected at CO_2 seeps (pH_T 7.2) were generally lower than samples from the reference site (pH_T 8.0) (Tukey's LSD tests $p < 0.001$ for both September and November, Supplementary Table 16b), whereas they were consistently greater in *C. neritea* from CO_2 seeps than those living in normal conditions (Tukey's LSD tests, September: $p = 0.034$; November: $p < 0.001$, Supplementary Table 16b). *Nassarius corniculus* from high-CO_2 environments consistently maintained significantly lower calcification rates than those at the reference site even when they were removed from elevated CO_2 and cultured at pH_T 8.0 (Fig. 3b,c; overall GLM $p < 0.001$, Supplementary Table 17a; Tukey's LSD tests for both months separately, $p < 0.001$, Supplementary Table 17b), showing adaptation to acidified environments rather than plasticity of calcification in response to pH conditions. Our findings add to a growing body of evidence that calcification responses to acidification are both species specific[28], which is unsurprising as there can be a great deal of biological control over calcification[18], and adaptive rather than plastic[19].

The mechanisms that underpin calcification responses to ocean acidification are a matter of debate[18]. Many benthic organisms calcify in waters that are undersaturated with carbonate, although they may incur elevated energetic costs resulting in reduced fitness, growth, reproduction and response to predators. Limpets that live in high-CO_2 areas[21] are not dwarfed, but counteract shell dissolution by upregulating their calcification rates[20], and therefore have to meet the higher energetic cost required to calcify[18]. Other organisms in which calcification rates are affected at high p_{CO_2} levels (including economically important shellfish such as clams, oysters and mussels[29]) may adapt ocean acidification through reductions in size[19], therefore reducing the total whole-animal energy demand but at the same time increasing the mass-specific energy demand necessary to maintain calcification and compensate for calcium carbonate dissolution.

We found that metabolic oxygen consumption corrected for body mass (mass-adjusted MO_2), which is the best descriptor of the animal's metabolic/maintenance costs, was significantly higher at CO_2 seeps (pH_{NBS} 6.5) compared with the samples from a reference site (pH_{NBS} 8.1) for both *C. neritea* and *N. corniculus* (Fig. 3d; GLM $p < 0.001$, Supplementary Table 18a); however, because of dwarfing, whole animal metabolic demands were significantly lower at the CO_2 seeps in both species (Fig. 3e; GLM $p < 0.001$, Supplementary Table 18b). Size reduction may compensate for loss of metabolic efficiency at high CO_2, in addition to the mass specific increased costs of maintenance. Our results support the conclusions of ref. 19, which demonstrated both physiological acclimatization and metabolic adaptation to high p_{CO_2} and reductions in size in seep-associated populations of benthic polychaetes. We therefore corroborate the observation that p_{CO_2}-tolerant species seem more likely to compensate for environmentally stressful conditions by elevating metabolic rates at the expense of growth.

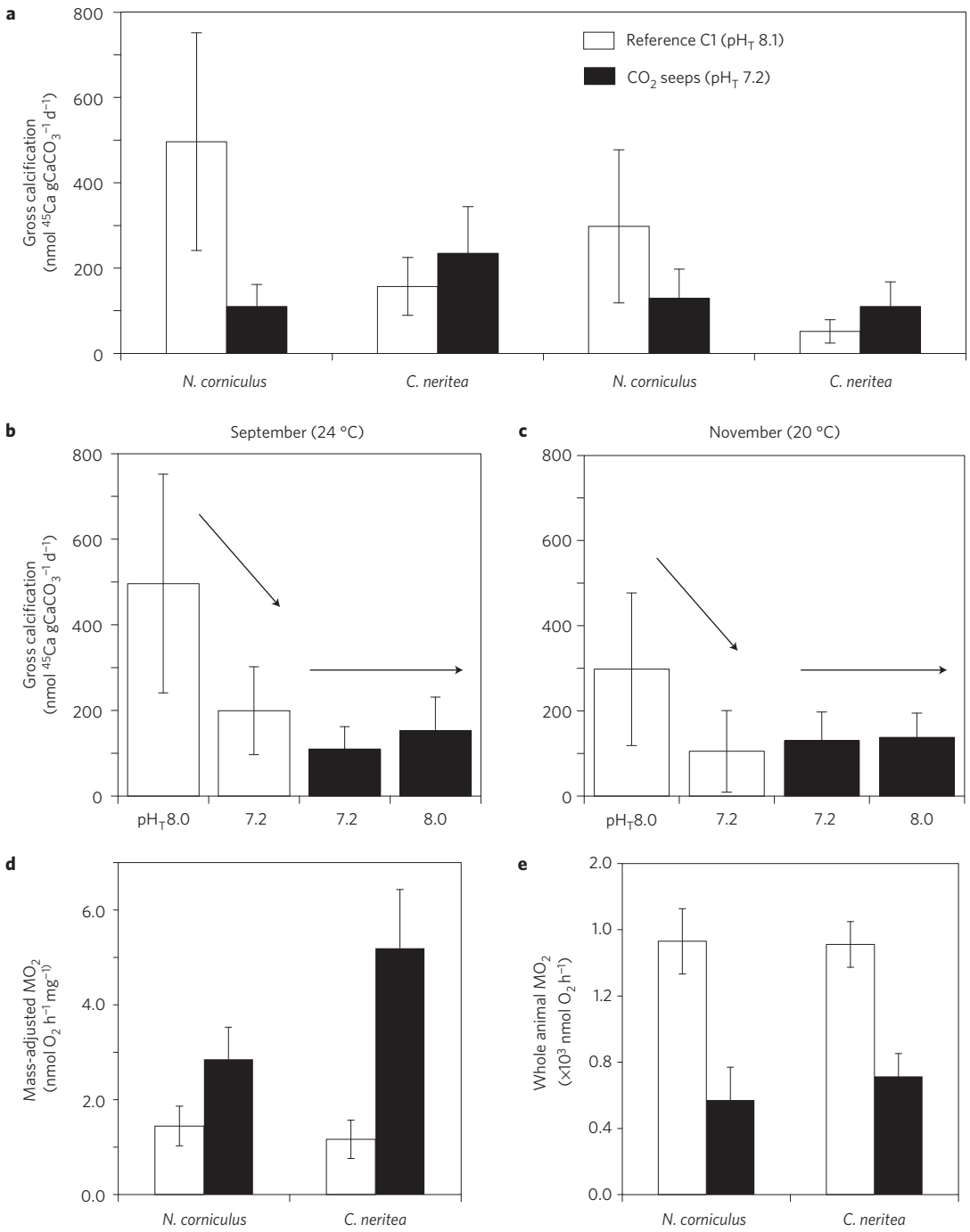

Figure 3 | Gross calcification and metabolic oxygen consumption in *N. corniculus* and *C. neritea* across normal and acidified sites. a, Gross calcification (GC, given in) in September and November at pH measured at collection sites. **b**,**c**, GC of *N. corniculus* in September (**a**) and November (**b**) using a two-way orthogonal experimental design (acclimation state/Origin × pH) to measure the response of samples collected within the seeps and at reference sites and incubated at crossed pH treatments. Arrows show the GC change on samples incubated at pH of collection (CO_2 seeps or reference site C1) and the pH of the incubation (pH$_T$ 8.0 and 7.2). For September, numbers of *N. corniculus* and *C. neritea* were $n=14$–39 and $n=16$. For November, numbers of *N. corniculus* and *C. neritea* were $n=16$–30 and $n=16$–20 (see Supplementary Information). Data are means ± s.d. **d**,**e**, Oxygen uptake as an index of metabolic rates (MO_2) expressed as body-mass-adjusted MO_2 (**d**) and whole-animal MO_2 (**e**). Sample replicates are $n=9$; data are means ± s.d.

Instead of being merely a result of changes in energy partitioning leading to changes in the rates of growth/calcification, small body size may be of selective advantage in maintaining mass-specific rates of energy consumption within an energy-limited environment. This would allow individuals to consume less energy, trading off growth and calcification against lifetime reproductive output. Furthermore, this would have conferred additional advantages during past global warming crises where changes in productivity may have impacted the availability of food resources[2,3,9].

Geologic evidence for mass extinctions associated with elevated CO_2 levels provides a stark warning for today, as the current rate of ocean acidification and warming is more rapid than during historical events and is acting synergistically with other global anthropogenic stressors. Understanding the ramifications of the

potential current mass extinction is limited, as we do not know which organisms will be able to evolve and how they might adapt to survive these changes. Organisms that have been exposed over multiple generations to elevated CO_2 levels provide valuable insights both into changes we can expect in marine ecosystems as CO_2 emissions continue to rise unchecked, and into past mass extinctions; not only do they demonstrate a similar magnitude and direction of body size change as fossil organisms, but they also reveal the physiological advantages of dwarfing. It is critical that we understand the mechanisms by which certain species survive chronic exposure to elevated CO_2, as emissions of this gas are already having adverse effects on marine food webs and putting food security at risk[30].

Methods

Methods and any associated references are available in the online version of the paper.

Received 20 November 2014; accepted 23 March 2015; published online 20 April 2015

References

1. Mora, C. *et al.* Biotic and human vulnerability to projected changes in ocean biogeochemistry over the 21st century. *PLoS Biol.* **11,** e1001682 (2013).
2. Benton, M. J. & Twitchett, R. J. How to kill (almost) all life: The end-Permian extinction event. *Trends Ecol. Evol.* **18,** 358–365 (2003).
3. Kidder, D. L. & Worsley, T. R. Phanerozoic Large Igneous Provinces (LIPs), HEATT (HalineEuxinic Acidic Thermal Transgression) episodes, and mass extinctions. *Palaeogeogr. Palaeoclimatol. Palaeoecol.* **295,** 162–191 (2010).
4. McElwain, J. C., Beerling, D. J. & Woodward, F. I. Fossil plants and global warming at the Triassic–Jurassic boundary. *Science* **285,** 1386–1390 (1999).
5. Twitchett, R. J. The Lilliput effect in the aftermath of the end-Permian extinction event. *Palaeogeogr. Palaeoclimatol. Palaeoecol.* **252,** 132–144 (2007).
6. Morten, S. D. & Twitchett, R. J. Fluctuations in the body size of marine invertebrates through the Pliensbachian–Toarcian extinction event. *Palaeogeogr. Palaeoclimatol. Palaeoecol.* **284,** 29–38 (2009).
7. Urbanek, A. Biotic crises in the history of Upper Silurian graptoloids: A palaeobiological model. *Historical Biol.* **7,** 29–50 (1993).
8. Fraiser, M. L. & Bottjer, D. J. Elevated atmospheric CO_2 and the delayed biotic recovery from the end-Permian mass extinction. *Palaeogeogr. Palaeoclimatol. Palaeoecol.* **252,** 164–175 (2007).
9. Kidder, D. L. & Worsley, T. R. Causes and consequences of extreme Permo-Triassic warming to globally equable climate and relations to the Permo-Triassic extinction and recovery. *Palaeogeogr. Palaeoclimatol. Palaeoecol.* **203,** 207–237 (2004).
10. Retallack, G. J. & Jahren, A. H. Methane release from igneous intrusion of coal during Late Permian extinction events. *J. Geol.* **116,** 1–20 (2008).
11. Veron, J. E. N. Mass extinctions and ocean acidification: Biological constraints on geological dilemmas. *Coral Reefs* **27,** 459–472 (2008).
12. Chapman, M. E. & Payne, J. L. Acidification, anoxia, and extinction: A multiple logistic regression analysis of extinction selectivity during the Middle and Late Permian. *Geology* **39,** 1059–1062 (2011).
13. Hautmann, M. Effect of end-Triassic CO_2 maximum on carbonate sedimentation and marine mass extinction. *Facies* **50,** 257–261 (2004).
14. Metcalfe, B., Twitchett, R. J. & Price-Lloyd, N. Size and growth rate of 'Lilliput' animals in the earliest Triassic. *Palaeogeogr. Palaeoclimatol. Palaeoecol.* **308,** 171–180 (2011).
15. Payne, J. L. Evolutionary dynamics of gastropods size across the end-Permian extinction and through the Triassic recovery interval. *Paleobiology* **31,** 269–290 (2005).
16. Palmer, A. R. Calcification in marine molluscs: How costly is it? *Proc. Natl Acad. Sci. USA* **89,** 1379–1382 (1992).
17. McCulloch, M., Falter, J., Trotter, J. & Montagna, P. Coral resilience to ocean acidification and global warming through pH up-regulation. *Nature Clim. Change* **2,** 623–627 (2012).
18. Findlay, H. S. *et al.* Comparing the impact of high CO_2 on calcium carbonate structures in different marine organisms. *Mar. Biol. Res.* **7,** 565–575 (2011).
19. Calosi, P. *et al.* Adaptation and acclimatization to ocean acidification in marine ectotherms: An *in situ* transplant experiment with polychaetes at a shallow CO_2 vent system. *Phil. Trans. R. Soc. B* **368,** 20120444 (2013).
20. Rodolfo-Metalpa, R. *et al.* Coral and mollusc resistance to ocean acidification adversely affected by warming. *Nature Clim. Change* **1,** 308–312 (2011).
21. Hall-Spencer, J. M. *et al.* Volcanic carbon dioxide vents show ecosystem effects of ocean acidification. *Nature* **454,** 96–99 (2008).
22. Fabricius, K. E. *et al.* Losers and winners in coral reefs acclimatized to elevated carbon dioxide concentrations. *Nature Clim. Change* **1,** 165–169 (2011).
23. Boatta, F. *et al.* Geochemical survey of Levante Bay, Vulcano Island (Italy), a natural laboratory for the study of ocean acidification. *Mar. Pollut. Bull.* **73,** 485–494 (2013).
24. Southward, A. J. *et al.* Behaviour and feeding of the nassariid gastropod *Cyclopeneritea*, abundant at hydrothermal brine seeps off Milos (Aegean Sea). *J. Mar. Biol. Assoc. UK* **77,** 753–771 (1997).
25. Palazzi, S. *Nassarius corniculus* (Olivi, 1792): Un suo interessante ecotipo delle isole circumsiciliane. *Boll. Malacol.* **23,** 259–262 (1987).
26. Tunnicliffe, V. *et al.* Survival of mussels in extremely acidic waters on a submarine volcano. *Nature Geosci.* **2,** 344–348 (2009).
27. Saether, K. P., Little, C. T. S. & Campbell, A. A new fossil provannid gastropod from Miocene hydrocarbon seep deposits, Ease Coast Basin, North Island, New Zealand. *Acta Palaeontol. Pol.* **55,** 507–517 (2010).
28. Ries, J. B., Cohen, A. L. & Mccorkle, D. C. Marine calcifiers exhibit mixed responses to CO_2-induced ocean acidification. *Geology* **37,** 1131–1134 (2009).
29. Sanford, E. *et al.* Ocean acidification increases the vulnerability of native oysters to predation by invasive snails. *Proc. R. Soc. B* **281,** 20132681 (2014).
30. Branch, T. A. *et al.* Impacts of ocean acidification on marine seafood. *Trends Ecol. Evol.* **28,** 178–186 (2012).

Acknowledgements

We thank F. Houlbreque, J-F. Comanducci and F. Oberhänsli for their help during radiotracer experiments. We also thank H. Graham, D. Small and C. Bertolini for assisting in the field. The International Atomic Energy Agency is grateful to the Government of the Principality of Monaco for the support provided to its Environment Laboratories. This work contributes to the EU 'Mediterranean Sea acidification under a changing climate' project (MedSeA; grant agreement 265103) and the NERC UK Ocean Acidification Research Programme (Grant no. NE/H02543X/1). S.P.S.R. was funded by a NERC UK Ocean Acidification Research Programme AVA fellowship. This is UMR ENTROPIE scientific contribution n. 028.

Author contributions

V.G. and R.R-M. designed the study and wrote the paper in collaboration with M.M., A.F., R.J.T., S.P.S.R. and J.M.H-S.; V.G. and D.P. performed scanning electronic microscopy analyses; R.R-M. performed gastropod radiotracer incorporation; S.P.S.R. and M.M. performed metabolic rate experiments; A.F. performed statistical analysis; M.M., D.S. and L.B. helped during sampling. J.M.H-S. conceived the overall seep project. All authors read and commented on the manuscript.

Additional information

Supplementary information is available in the online version of the paper. Reprints and permissions information is available online at www.nature.com/reprints. Correspondence and requests for materials should be addressed to V.G. or R.R-M.

Competing financial interests

The authors declare no competing financial interests.

Methods

Sampling sites. For shell morphometric parameters, scanning electronic microscopy analyses, gross calcification and metabolic rate measurements, *Nassarius corniculus* and *Cyclope neritea* were collected in September and November 2011 at CO_2 seeps off Vulcano Island (northern Sicily, Aeolian Archipelago, Tyrrhenian Sea), and at reference site C1 in the Stagnone of Marsala (western Sicily; Supplementary Fig. 1). Specimens of *N. corniculus* were also collected at two other reference sites—Lampedusa Island (C2; southern Sicily) and San Giovanni Li Cuti (C3; eastern Sicily)—and their shell morphometric parameters were measured.

Seawater carbonate chemistry. Seawater carbonate chemistry variations at CO_2 seeps were frequently measured during our previous studies (for example, ref. 22). Total alkalinity (A_T) and pH expressed in total scale (pH_T) were measured during the 2–3 day sample collections in September and November 2011, and routinely during aquarium experiments (Supplementary Information). Parameters of the carbonate system were calculated from pH_T, mean A_T, temperature and mean salinity (38) using the free-access CO_2SYS package. pH variation at CO_2 seeps was measured over a 24-h cycle using a multiparametric probe (556 MPS YSI) positioned at 2 m depth.

Shell morphometric and scanning electron microscopy analyses. Samples were preserved in 70% ethanol after collection. Morphometric parameters, such as total shell height (Ht), shell maximum width (W), shell width at the suture between last and penultimate whorl (Ws), last whorl height (Hlw), aperture height (Ha) and thickness of the outer lip (Olt), were measured on adult *C. neritea* and *N. corniculus* shells collected at CO_2 seeps and the three reference sites C1–C3 using a stereomicroscope. *Nassarius corniculus* shell macro- and microstructures were investigated using a LEO 420 scanning electron microscope on samples from Vulcano and the reference site C1.

Aquarium experiments and gross calcification (GC). After collection, both in September and November 2011, samples were transported to the IAEA-MESL laboratory in Monaco. They were maintained in flow-through aquaria containing sediments collected from sampling sites. *C. neritea* were divided per site of collection at field pH (sites C1, pH_T 8.0 and CO_2 seep, pH_T 7.2–7.3) whereas *N. corniculus* were incubated using a two-way orthogonal experimental design (acclimation state/Origin × pH) to measure the GC rates of samples collected within and outside the vents at crossed pH treatments. Half of the *N. corniculus* from both sites were incubated at temperature and pH conditions similar to *in situ* values (CO_2 seep: pH_T 7.2–7.3; site C1: pH_T 8.0; Supplementary Table 1), whereas the remaining specimens were incubated at pH_T 7.2–7.3 and pH_T 8.0 for specimens from reference and CO_2 seep sites, respectively. After two weeks, samples were transferred in separated 6 litre aquaria (two to three replicate tanks for each site/pH treatment) and their GC were measured with the radiotracer ^{45}Ca (Supplementary Information).

Metabolic rates. Metabolic oxygen consumption (MO_2) was determined for *C. neritea* and *N. corniculus* from both CO_2 seeps and reference site C1 within 24 h of collection. During individual incubations, gastropods were allowed to acclimatize to the respirometry chambers, receiving fully oxygenated water from their site of collection at pH_{NBS} 6.5 or pH_{NBS} 8.1 for individuals collected at CO_2 seeps and reference site C1, respectively. After 1 h acclimatization the chambers were closed, measurement run for another hour and the decrease in p_{O_2} within each respirometer stop-flow chamber measured using a polarographic O_2 electrode (E-5046 electrode, Radiometer) connected to an oxygen meter (Strathkelvin Oxygen Meter 781). Then, specimens were killed to measure their shell-free wet-body mass for use as a covariate in GLM analysis of MO_2.

Statistical analysis. Univariate data on shell morphometric parameters (Supplementary Information), GC and metabolic rates were analysed using GLM in SPSS 21.0; data are presented as mean ± s.d. Pair-wise comparisons between treatments were performed using a priori contrasts based on estimated marginal means and Tukey's LSD tests. Conformity to assumptions of GLM was confirmed by homogeneity of variances testing and inspection of analytical residuals; transformations were used when necessary. Multivariate analyses of overall organism shape were conducted using PERMANOVA in PRIMER version 6.1 (see Supplementary Information for all details and results).